The Journal of Neuroscience, October 15, 1996, *16*(20):6414–6423

Excitatory GABA Responses in Embryonic and Neonatal Cortical Slices Demonstrated by Gramicidin Perforated-Patch Recordings and Calcium Imaging

David F. Owens, Leslie H. Boyce, Marion B. E. Davis, and Arnold R. Kriegstein

Department of Neurology and The Center for Neurobiology and Behavior, College of Physicians and Surgeons of Columbia University, New York, New York 10025

Gramicidin perforated-patch-clamp recordings in brain slices were used to obtain an accurate assessment of the developmental change in the $GABA_A$ receptor reversal potential (E_{GABA_A}) in embryonic and early postnatal rat neocortical cells including neuroepithelial precursor cells, cortical plate neurons, and postnatal neocortical neurons. Our results demonstrate that there is a progressive negative shift in E_{GABA_A}, with the most positive values found in the youngest cortical precursor cells. At the early stages of neocortical development, E_{GABA_A} is determined by the chloride (Cl^-) gradient, and the internal chloride concentration ($[Cl^-]_i$) decreases with development. E_{GABA_A} is positive to the resting potential, indicating that GABA serves to depolarize developing neocortical cells. Consistent with this conclusion, $GABA_A$ receptor activation with muscimol was found to increase the internal calcium concentration ($[Ca^{2+}]_i$) in both embryonic and early postnatal neocortical cells through the activation of voltage-gated calcium channels (VGCCs). Postnatal cells exhibit spontaneous postsynaptic synaptic currents, which are eliminated by bicuculline methiodide (BMI) but not glutamate receptor antagonists and reverse at the Cl^- equilibrium potential. Likewise, brief spontaneous increases in $[Ca^{2+}]_i$, sensitive to BMI and TTX, are observed at the same ages, suggesting that endogenous synaptic $GABA_A$ receptor activation can depolarize cells and activate VGCCs. These results suggest that $GABA_A$ receptor-mediated depolarization may influence early neocortical developmental events, including neurogenesis and synaptogenesis, through the activation of Ca^{2+}-dependent signal transduction pathways.

Key words: cortical development; GABA; intracellular calcium; perforated-patch recording; neocortex; synaptogenesis

GABA is the principal inhibitory neurotransmitter in the adult neocortex. It has been shown recently that $GABA_A$ receptors are expressed early in cortical development on proliferating neuroepithelial cells in the embryonic ventricular zone (VZ) (LoTurco and Kriegstein, 1991; LoTurco et al., 1995) as well as on immature neurons in the cortical plate (CP) (LoTurco and Kriegstein, 1991; Araki et al., 1992; Laurie et al., 1992; Poulter et al., 1992). Several studies have reported that $GABA_A$ receptor activation depolarizes embryonic neuroblasts and neonatal cortical neurons (Luhmann and Prince, 1991; LoTurco et al., 1995). Likewise, GABA application has been shown to increase $[Ca^{2+}]_i$ in developing neocortical cells by activation of voltage-gated Ca^{2+} channels (Yuste and Katz, 1991; Lin et al., 1994; LoTurco et al., 1995). GABA also can depolarize adult neocortical neurons when applied to distal dendrites (Connors et al., 1988; Staley et al., 1995). However, the mechanism underlying depolarization may be different in immature and adult cortical neurons. $GABA_A$-mediated depolarization in immature neurons is thought to be attributable to a high $[Cl^-]_i$, possibly maintained by unopposed inward Cl^- transport (Luhmann and Prince, 1991; LoTurco et al., 1995). In more mature neurons, GABA depolarization might be attributable to a high $[Cl^-]_i$ in dendritic compartments (Deisz and Luhmann, 1995) or could result from conductance of another anion through the $GABA_A$ channel such as bicarbonate (Staley et al., 1995). Because the role of GABA during early stages of corticogenesis is likely to depend on its effect on membrane potential, it is important to clarify the mechanism of GABA depolarization in embryonic and neonatal cortical neurons. To study cellular chloride ion gradients *in situ*, we used a perforated-patch-recording method applied to slices and explants of embryonic and neonatal rat cortex.

The $GABA_A$ receptor is primarily a chloride (Cl^-) ionophore (Bormann et al., 1987); therefore, an accurate characterization of the $GABA_A$-mediated depolarization in developing neocortical cells requires an intact $[Cl^-]_i$. Sharp electrode recording, which may not significantly alter the intracellular ionic composition, cannot be applied to very small, fragile cells. Whole-cell patch-clamp recording is well-suited to recording from small cells but perturbs intracellular ionic concentrations by dialyzing cytoplasmic contents. The method of perforated-patch recording can circumvent these limitations. The most commonly used ionophores (i.e., amphotericin B and nystatin), however, create pores that are permeable to Cl^- (Marty and Finkelstein, 1975; Horn and Marty, 1988). In contrast, gramicidin has been shown to form membrane pores that are exclusively permeable to monovalent cations and small, uncharged molecules (Hladky and Haydon, 1972; Myers and Haydon, 1972), thus allowing for patch-clamp recordings that leave the $[Cl^-]_i$ undisturbed (Abe et al., 1994; Ebihara et al., 1995; Kyrozis and Reichling, 1995). To better understand the role of GABA during cortical development, we

Received May 17, 1996; revised July, 18, 1996; accepted July 24, 1996.

This work was supported in part by Research Grant FY95-0879 from the March of Dimes Birth Defects Foundation, National Institutes of Health Grant NS 21223, and Neurological Sciences Academic Development Award NS01698 to L.H.B. We thank Cristovao de Albuquerque, Amy MacDermott, and Gareth Tibbs for helpful comments on this manuscript, and Alexander Flint for helpful comments and assistance with computer graphics.

Correspondence should be addressed to Dr. Arnold R. Kriegstein, Department of Neurology, College of Physicians and Surgeons of Columbia University, 630 West 168th Street, P.O. Box 31, New York, NY 10032.

used the gramicidin perforated-patch technique to study the membrane effects of $GABA_A$ receptor activation in populations of embryonic and neonatal cortical cells.

MATERIALS AND METHODS

Tissue preparation. Gravid rats (Sprague Dawley) were anesthetized with an intraperitoneal injection of ketamine (50 mg/kg), and embryos were exposed by cesarean section. Animals were decapitated, and heads were placed immediately in iced artificial CSF (ACSF) containing (in mM): 124 NaCl, 5 KCl, 1.25 NaH_2PO_4, 2 $MgSO_4$, 2 $CaCl_2$, 26 $NaHCO_3$, and 10 glucose, oxygenated with 95% O_2/5% CO_2, pH 7.4. Cerebral hemispheres or whole brains were removed, and for experiments requiring brain slices, tissue was embedded in warm (28–30°C) 1% low-melting agarose (Fisher Scientific, Fair Lawn, NJ) in ACSF, hardened on ice, and sliced into coronal sections with a vibratome (300–400 μm). For some experiments, telencephalic hemispheres were not sliced but prepared as slabs of neocortex by trimming off the hippocampus and striatal anlage. Postnatal rat pups [postnatal age 0 (P0) to P2] were anesthetized by hypothermia or intraperitoneal injection of ketamine (50 mg/kg) and rapidly decapitated. Brains were removed and placed in ice-cold ACSF oxygenated with 95% O_2/5% CO_2 and sliced coronally with a vibratome (300–400 μm). Slices were confined to the sensorimotor regions of the cortex. Tissue was kept in oxygenated ACSF at room temperature (RT) (21–23°C) for at least 1 hr before recording.

Electrophysiological recordings. Patch-clamp recordings were obtained at RT from cells in both slices and slabs of neocortex continuously superfused with 95% O_2/5% CO_2 oxygenated ACSF. Methods for *in situ* patch-clamp recording have been described previously (Blanton et al., 1989). Briefly, electrodes (8–12 MΩ) were lowered onto the surface of a cortical slice or explant and slowly advanced until a resistance increase was detected (10–50 MΩ), after which a suction pulse was applied immediately to form a tight seal (2–40 GΩ). To establish whole-cell recording, additional suction was applied to rupture the underlying plasma membrane. Perforated-patch recordings (Abe et al., 1994; Ebihara et al., 1995; Kyrozis and Reichling, 1995) were obtained using identical methods, except mechanical rupture of the plasma membrane was omitted. The progress of perforation was evaluated by monitoring the decrease in the membrane resistance. Drugs were applied after the membrane resistance had stabilized; this usually took from 1 to 10 min. Gramicidin (Sigma, St. Louis, MO) was dissolved in dimethylsulfoxide (DMSO) (Sigma) (1–2 mg/ml) then diluted in the pipette filling solution to a final concentration of 0.2–5 μg/ml. In some experiments, perforated-patch recordings were converted to whole-cell recordings by applying suction to rupture the underlying plasma membrane. For the majority of recordings, patch electrodes were filled with a solution containing (in mM): 100 CsCl, 30 Cs gluconate, 10 HEPES, pH 7.3, 2 $CaCl_2$, and 11 EGTA. To test different concentrations of Cl^- in the pipette solution ($[Cl^-]_p$), whole-cell recordings were made with gluconate substituted for Cl^- in the filling solution. In some whole-cell recordings, a KCl filling solution was used containing (in mM): 130 KCl, 5 NaCl, 0.4 $CaCl_2$, 1 $MgCl_2$, 10 HEPES, pH 7.3, and 1.1 EGTA. Liquid junction potentials for the CsCl and KCl filling solutions (Neher, 1992) were −4.7 and −3.4 mV, respectively. In CsCl filling solutions in which gluconate substituted for Cl^-, liquid junction potentials were −6.8 and −9.1 mV for a 54 mM Cl^- solution and a 20 mM Cl^- solution, respectively. Data from experiments that tested different concentrations of $[Cl^-]_p$ were corrected for liquid junction potentials (see Fig. 4*C*). When using voltage ramps, recordings were digitized and analyzed with pClamp software (Axon Instruments, Foster City, CA). The voltage-ramp protocol consisted of stepping the cell from a holding potential of −60 to +20 or +40 mV for 80 msec, then changing the voltage to −100 mV at a rate of 150 mV/sec. *I–V* curves were plotted after subtracting the control response obtained in ACSF from the response obtained during agonist application. In these experiments, the $GABA_A$ reversal potential was defined as the *x*-intercept value of the muscimol-induced current. GABA (30 μM) was applied with the membrane held at a series of potentials. Peak current responses for each voltage were plotted, and the data were fit using CA-Cricket Graph III software (Computer Associates). The GABA-mediated reversal potential was defined as the *x*-intercept value of the fit. Unless noted, the bath ACSF in experiments using ramp voltage clamp contained La^{3+} (30 μM) to block voltage-gated calcium channels (VGCCs) (Reichling and MacDermott, 1991). In all experiments, TTX (2 μM) was added if voltage-activated Na^+ currents were detected, and potassium (K^+) conductances were blocked by cesium (Cs^+) (130 mM) in the pipette filling solution. In some experiments, recordings were performed in a bicarbonate-free, HEPES-buffered saline solution containing (in mM): 124 NaCl, 5 KCl, 1.25 NaH_2PO_4, 26 HEPES, 2 $MgSO_4$, 2 $CaCl_2$, and 10 glucose, pH 7.4, bubbled with 100% O_2. For all experiments, average values are expressed as mean ± SEM.

Calcium imaging in brain slices using fluo-3. Coronal slices were prepared as described above. Cells were loaded in the dark with the Ca^{2+} indicator dye fluo-3 by immersion for 60 min in ACSF containing the acetomethylester form of fluo-3 (fluo-3AM) (10 μM) followed by ACSF wash. Slices were placed in a perfusion chamber on the stage of a Zeiss Axiovert microscope (40×, numerical aperture 0.75 objective) with a Bio-Rad (Hercules, CA) MRC-600 argon laser scanning confocal attachment. Excitation was at 488 nm, and emissions were collected using a 515 nm long-pass emission filter. Neutral density filters were used to filter the argon laser light to 1% to minimize photobleaching. Images were acquired at 1.0 sec/frame, and two frames were averaged for each image. Considering the 2 sec download time, images were acquired at either 4.0 sec/image or 5.0 sec/image. Images were acquired on an IBM compatible computer running Comos acquisition software (Bio-Rad). Fluorescence micrographs were digitized, and relative changes in $[Ca^{2+}]_i$ from randomly selected cells were measured using the public domain National Institutes of Health (NIH) Image program (written by Wayne Rasband at NIH) on a Macintosh 7200 computer. Data are expressed as a change in fluorescence over baseline fluorescence ($\Delta F/F$). A microscopic field was visualized and perfused with drug-free medium while three images were obtained and averaged to obtain the baseline value *F*. Each subsequent image during drug application and washout was processed and expressed as a change in fluorescence over baseline fluorescence by $\Delta F/F$. For experiments measuring spontaneous $[Ca^{2+}]_i$ fluctuation, *F* was defined as the frame with the minimum level of fluorescence. In solutions that used Cd^{2+}, 2 mM HEPES replaced NaH_2PO_4 in the ACSF. Average values are expressed as mean ± SEM.

Pharmacological agents. Muscimol, furosemide, bicuculline methiodide (BMI), lanthanum (La^{3+}), cadmium (Cd^{2+}), and TTX were obtained from Sigma; GABA, 6-cyano-7-nitroquinoxaline-2,3-dione (CNQX), and 2-amino-5-phosphonopentanoic acid (AP-5) were obtained from RBI (Natick, MA). In electrophysiological experiments, GABA, muscimol, BMI, and AP-5 were applied by focal puffer application (DAD-12 Superfusion System, ALA Scientific Instruments, Westbury, NY). Furosemide, La^{3+}, CNQX, and TTX were bath-applied. In Ca^{2+} imaging studies, all drugs were bath-applied. Drugs were kept as concentrated stock solutions at −20°C (muscimol, BMI, CNQX, AP-5, Cd^{2+}, and GABA) or 4°C (La^{3+} and TTX) and diluted to the desired concentration on the day of the experiment. Furosemide was dissolved directly in ACSF. Fluo-3AM was obtained from Molecular Probes (Eugene, OR).

RESULTS

Gramicidin perforated-patch recording in brain slices

Comparing perforated-patch with whole-cell recording in the same cell confirmed the importance of $[Cl^-]_i$ in determining GABA-mediated responses. An example is shown in Figure 1. A gramicidin perforated-patch recording from an embryonic day 19 (E19) CP neuron was obtained, and GABA (30 μM) was applied focally with the membrane potential held at −60 mV and again at −30 mV (Fig. 1*A*,*B*, *left traces*). The perforated patch was converted into a whole-cell recording by applying suction, and GABA was reapplied (Fig. 1*A*,*B*, *right traces*). As shown in Figure 1*C*, the reversal potential for the perforated-patch recording was approximately −40 mV. In the whole-cell configuration, the reversal potential was ~0 mV, close to the potential predicted by the Nernst equation (i.e., −6.2 mV), given the $[Cl^-]_p$ and assuming complete exchange with the cell cytoplasm. These data confirm that the gramicidin perforated-patch method does not allow Cl^- to cross the patch membrane.

E_{GABA_A} shifts to more negative potentials during development

Gramicidin perforated patches and muscimol (30 μM) application were used to determine the $GABA_A$ reversal potential in embryonic CP cells and early postnatal neocortical neurons. When

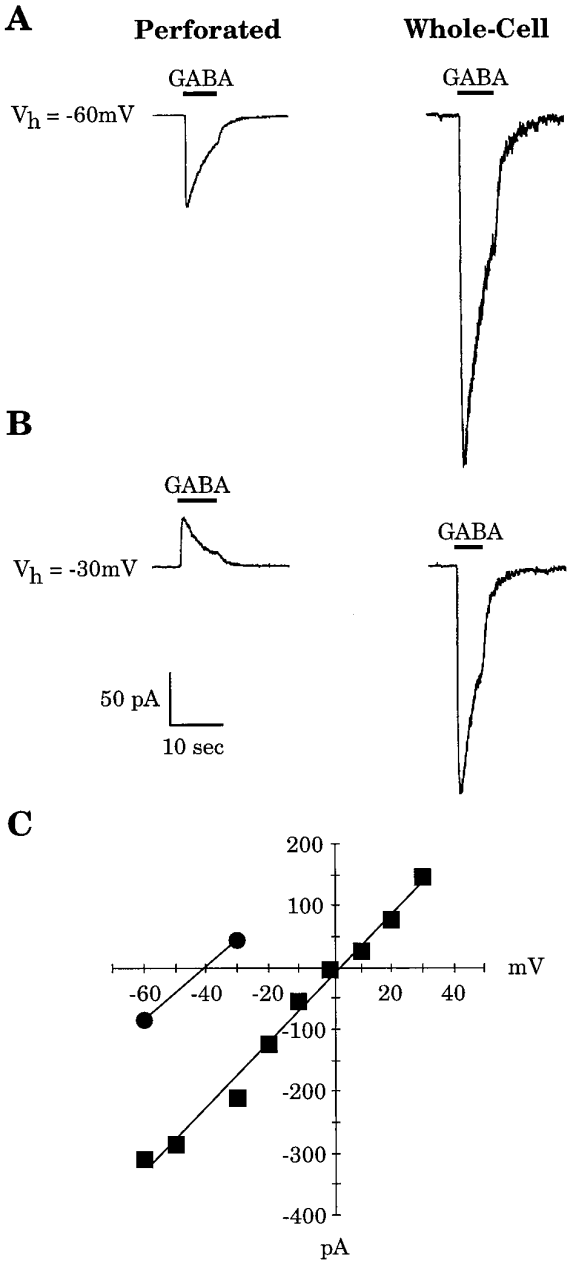

Figure 1. Comparison of gramicidin perforated-patch and whole-cell recordings in the same cell. *A*, *B*, The GABA (30 μM)-induced current was measured in an E19 CP cell at holding potentials (V_h) of −60 and −30 mV with a gramicidin perforated patch (traces at *left*). The recording was subsequently converted to a whole-cell recording, and GABA application was repeated (traces at *right*). *C*, The *I–V* relationship of GABA-induced currents is illustrated for both methods of recording. With the perforated patch, the GABA reversal potential was approximately −40 mV (*circles*), whereas in whole-cell mode, the reversal potential shifted to ~0 mV (*squares*), close to the value predicted by the Nernst equation.

cortical neurons undergo their final mitosis and migrate out of the VZ, they are small, electrically compact, have small processes, and are no longer coupled to VZ cells; these features provide favorable conditions for voltage-clamp studies. Figure 2*A* is an example of the voltage-ramp protocol applied to measure the $GABA_A$ reversal potential of an E19 CP cell, with the resulting current–voltage (*I–V*) curve shown in Figure 2*B*. For comparison, Figure 2*B* also shows the $GABA_A$ *I–V* curve derived from an E16 CP cell in whole-cell mode. Similar results were found in a second series of experiments that used the natural ligand GABA as agonist. GABA (30 μM) was applied focally to cells held at a series of membrane potentials, and *I–V* curves were constructed. Figure 2*C* shows an example of the *I–V* relationship of the GABA-induced response for a P2 neocortical neuron. The reversal potential is approximately −52 mV. In contrast, more mature neurons had more negative reversal potentials, as shown in Figure 2*D* for a P16 neuron with a GABA reversal potential of approximately −66 mV. GABA applications at P16 could produce complicated responses consisting of two or more phases (Fig. 2*D*, *inset*), presumably attributable to the maturation of the $GABA_B$ receptor subtype (Luhmann and Prince, 1991). When multiple components were present, the shortest latency peak current was the value used in the GABA *I–V* curve.

The earliest cells in the neocortex to express functional $GABA_A$ receptors are the proliferating neuroepithelial cells in the embryonic VZ (LoTurco et al., 1995). Because the proliferating VZ cells are electrically coupled to each other through gap junction channels (LoTurco and Kriegstein, 1991), the ability to voltage-clamp the membrane of a single cell and to measure E_{GABA_A} is limited by the large area of membrane composing a coupled cell cluster. There is evidence that at least some neonatal cortical neurons also are electrically coupled by dendrodendritic contacts to other cortical neurons in the first postnatal week (Connors et al., 1983; Peinado et al., 1993); nonetheless, voltage control over the soma and proximal dendritic membrane is much better in neonatal cortical neurons, where it is possible to obtain accurate reversal potentials for $GABA_A$ responses, than in VZ cells, where $GABA_A$ reversal potentials cannot be measured because of poor voltage control. Therefore, we used an indirect approach to estimate a lower limit value for the $GABA_A$ reversal potential in VZ cells. This consisted of measuring the peak depolarization produced by a saturating dose of muscimol using perforated-patch recordings. TTX (2 μM) and La^{3+} (30 μM) were added to the bathing solution to block voltage-gated Na^+ and Ca^{2+} currents, respectively, and Cs^+ (130 mM) was present in the electrode filling solution to block K^+ currents. The maximum depolarization, assuming blockage of voltage-dependent conductances, represents an indirect measurement of E_{GABA_A}. To determine the saturating concentration of muscimol, recordings were obtained from E16 VZ cells in current-clamp mode. In these cells, 50 μM and 100 μM muscimol produced nearly identical levels of depolarization (26.1 ± 3.6 mV for 50 μM muscimol and 26.5 ± 4.2 mV for 100 μM muscimol, $n = 6$), strongly suggesting that saturating responses could be obtained with 100 μM muscimol. Muscimol (100 μM) depolarized VZ cells to an average membrane potential of −32.2 ± 1.2 mV ($n = 6$). If intracellular Cs^+ was not able to reach all the cells in a coupled cluster, activation of voltage-activated K^+ currents in cells coupled to the recorded cell would lead to an underestimate of the true level of depolarization. This methodology, therefore, gives an estimate of the lower limit value for the $GABA_A$ reversal potential.

Considering the close agreement between the reversal potentials obtained with either GABA or muscimol as an agonist, these data were combined to provide a developmental time course for the changes in the reversal potential for the $GABA_A$ receptor-mediated current (Fig. 3*A*). Measurements made over a 3 week developmental period demonstrate that at embryonic stages, the average $GABA_A$ reversal potential was considerably less negative (−32.2 ± 1.2 mV for VZ cells at E16 and −38.2 ± 2.0 mV for CP cells at E16) than at later developmental periods (−61.3 ± 3.7 mV

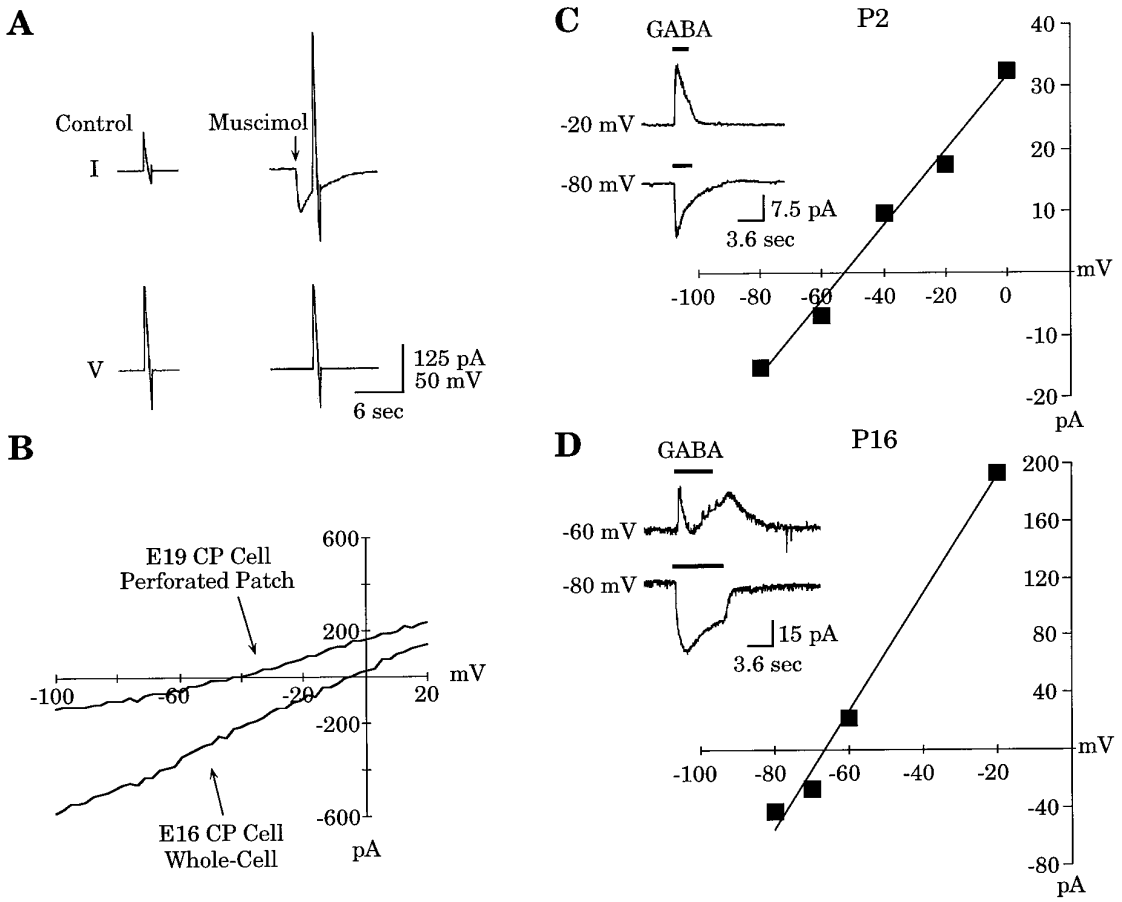

Figure 2. E_{GABA_A} was determined either by muscimol (30 μM) application and voltage ramps or by GABA (30 μM) application with the membrane held at a series of potentials. *A*, Voltage-ramp protocol applied to an E19 CP cell. *B*, The resulting *I–V* curve obtained from the recording in *A* after control-ramp subtraction. E_{GABA_A} is approximately −40 mV. For comparison, an *I–V* curve obtained from an E16 CP cell in whole-cell mode is shown. *C*, *I–V* relationship for a P2 neocortical neuron with a reversal potential of approximately −52 mV. The *inset* shows the GABA-induced current at two membrane potentials. Note the monophasic response at both holding potentials. *D*, *I–V* relationship for a P16 neocortical neuron with a reversal potential of approximately −66 mV. The *inset* shows the GABA-induced current at two membrane potentials. Note the greater complexity of the response at the −60 mV holding potential.

at P16). Because $GABA_B$ receptor-mediated responses are not readily detected until the second postnatal week (Luhmann and Prince, 1991), activation of both $GABA_A$ and $GABA_B$ receptors by GABA application probably would occur only for recordings performed at P16. However, when multiphasic GABA responses were observed at P16, measurements were taken from the peak of the initial phase of the response, which is mediated by $GABA_A$ receptors (Connors et al., 1988).

GABA responses are depolarizing because of high $[Cl^-]_i$

The effect of GABA or muscimol on the membrane potential of an individual neuron at a given age will depend both on the reversal potential for the agonist-induced current and on the resting membrane potential of the cell. To accurately measure E_{GABA_A}, our perforated-patch electrode solution contained Cs^+ to block voltage-dependent K^+ currents, but this also may bias the resting potential to more positive values. Therefore, resting potential measurements with a Cs^+-based pipette solution are difficult to interpret. To circumvent this problem, whole-cell recordings with KCl-filled electrodes were used to measure the resting membrane potential in the same cell populations in which E_{GABA_A} was determined. The average resting potential was −55.3 ± 1.2 mV in embryonic VZ cells (E15 and E17, n = 10), −65.0 ± 1.7 mV in embryonic CP cells (E18 and E19, n = 15), and −64.0 ± 4.3 mV in P3 cortical neurons (n = 6), as shown in Figure 3*A*. Given that these resting membrane potentials are more negative than E_{GABA_A} at the corresponding ages, $GABA_A$ receptor activation would produce membrane depolarization in these populations of embryonic and neonatal cortical cells.

Depolarizing GABA responses have been attributed to a number of different mechanisms including high $[Cl^-]_i$ (Luhmann and Prince, 1991), an increase in conductance to another anion such as bicarbonate (Kaila and Voipio, 1987; Kaila et al., 1989; Staley et al., 1995), or, possibly, a cation conductance (Andersen et al., 1980). Recent evidence in immature neurons has suggested that the Cl^- gradient may be the dominant contributor to $GABA_A$-induced depolarization (Reichling et al., 1994; Wang et al., 1994; Rohrbough and Spitzer, 1996). The contribution of the $[Cl^-]_i$ to E_{GABA_A}- and $GABA_A$-mediated depolarization in immature cortical neurons was investigated in several ways. First, whole-cell recordings were used to bias the $[Cl^-]_i$ to that of the pipette for three different $[Cl^-]_p$ values, and the muscimol-induced reversal potentials were measured. These values were compared with the reversal potential for Cl^- predicted by the Nernst equation. As

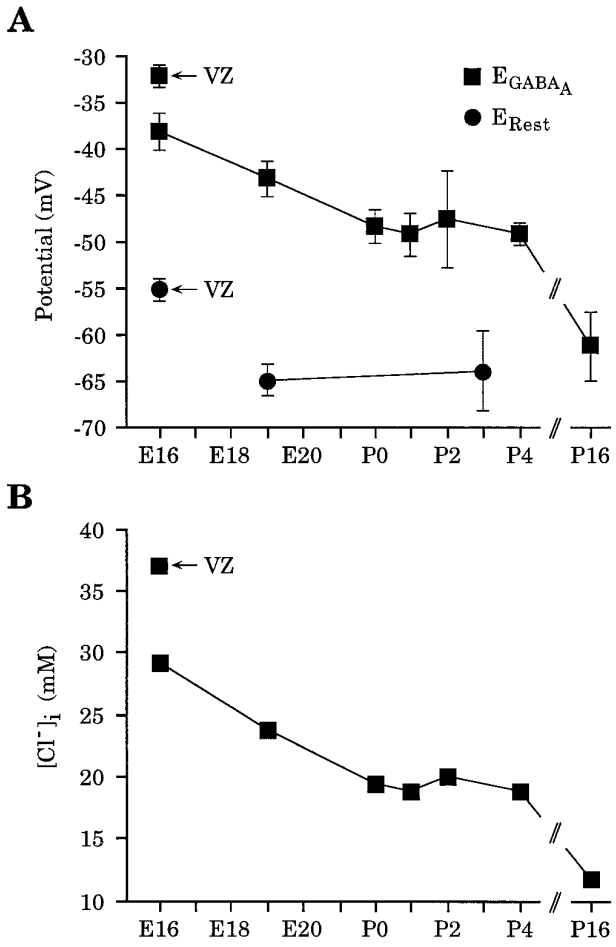

Figure 3. There is a progressive negative shift in E_{GABA_A} over development. *A*, Pooled reversal potentials derived from experiments using either GABA or muscimol as agonist. Also plotted are the resting membrane potentials (E_{Rest}) (see Results). Because resting potential measurements for VZ and CP cells were made on E15–E17 and E18–E19, respectively, their placement on the graph is approximate. For E_{GABA_A}, $n = 6$ for E16 VZ; $n = 14$ for E16 CP; $n = 22$ for E19 CP; $n = 3$ for P0; $n = 5$ for P1; $n = 3$ for P2; $n = 7$ for P4; $n = 5$ for P16. *B*, $[Cl^-]_i$ calculated from combined data in *A* using the Nernst equation. Values are as follows, E16 VZ, 37.0 mM; E16 CP, 29.2 mM; E19 CP, 23.8 mM; P0, 19.4 mM; P1, 18.8 mM; P2, 20.0 mM; P4, 18.8 mM; P16, 11.7 mM.

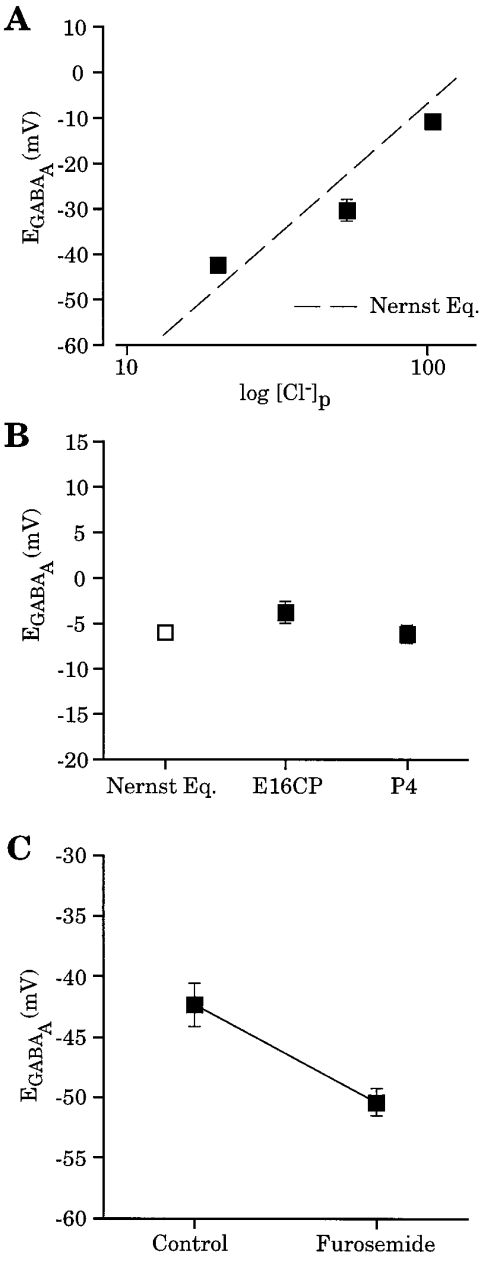

Figure 4. Cl^- gradient contributes significantly to E_{GABA_A}. *A*, Whole-cell recording with different $[Cl^-]_p$ (104 mM, $n = 3$; 52 mM, $n = 4$; 20 mM, $n = 3$) yielded reversal potentials comparable to those predicted by the Nernst equation (*dashed line*). Recordings were from P4 neocortical neurons; no La^{3+} was present in these experiments. These data were corrected for liquid junction potentials that were determined experimentally for each solution. *B*, Absence of a developmental shift in E_{GABA_A} using whole-cell recordings ($[Cl^-]_p = 104$ mM). E_{GABA_A} measured in E16 CP cells (-3.9 ± 1.3 mV, $n = 5$) and P4 neocortical cells (-6.4 ± 1.0 mV, $n = 3$) had values close to that predicted by the Nernst equation (-6.2 mV) (*open square*). *C*, Furosemide (2 mM) application produced a negative shift (-8.1 ± 0.9 mV, $n = 3$) in E_{GABA_A} determined with perforated-patch recordings from E16 CP cells. E_{GABA_A} for each cell was determined both before and after furosemide application, with the average values being -42.4 ± 1.8 and -50.4 ± 1.1 mV, respectively.

shown in Figure 4*A*, the experimental data fit the predicted values for the Cl^- gradient across the membrane, supporting the hypothesis that Cl^- is the principle ion mediating the $GABA_A$ receptor effect. Furthermore, despite the developmental shift in the $GABA_A$ reversal potential determined with perforated-patch recordings (see Fig. 3*A*), the $GABA_A$ reversal potential measured by whole-cell recording remained close to that predicted by the Nernst equation (Fig. 4*B*), confirming that $[Cl^-]_i$ is chiefly responsible for setting the $GABA_A$ reversal potential during this developmental period. To test whether bicarbonate ions are responsible for muscimol-induced inward current, perforated-patch recordings were obtained from E19 CP cells in bicarbonate-free, HEPES-buffered saline. Muscimol application still produced an inward current at a holding potential of -60 mV, a potential close to the average resting potential determined with KCl-filled electrodes. The average E_{GABA_A} measured under these conditions was -41.0 ± 5.1 mV ($n = 4$) (data not shown). This suggests that bicarbonate ions are not necessary for $GABA_A$-mediated inward currents at this age. Lastly, the $GABA_A$ reversal potential was determined using perforated-patch recordings, and then furosemide (2 mM), a Cl^- transport blocker, was applied to perturb the $[Cl^-]_i$. The muscimol-induced reversal potential in E16 CP

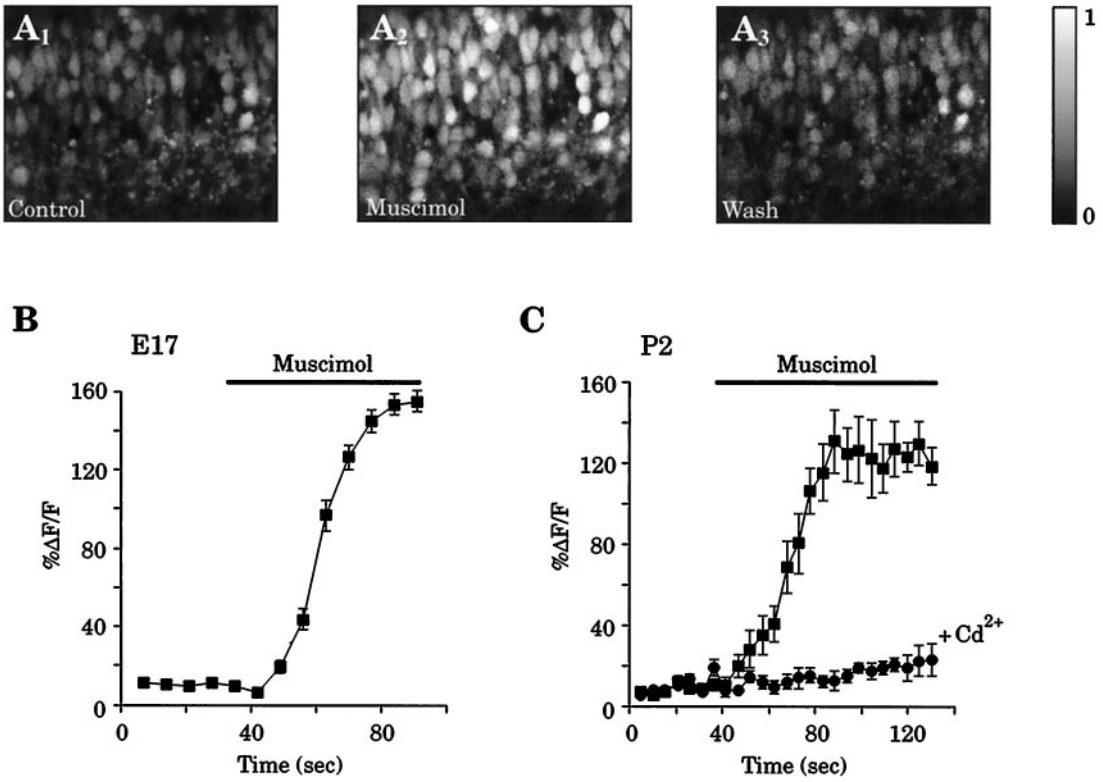

Figure 5. Muscimol (30 μM) produces increases in $[Ca^{2+}]_i$ in developing cortical cells. *A*, Confocal image of E17 CP cells loaded with the Ca^{2+} indicator fluo-3AM before (*1*), during (*2*), and after (*3*) application of muscimol (30 μM). Pial surface is to the *top* of the image. *B*, Eight cells were randomly chosen from the microscopic field in *A*, and the increases in $[Ca^{2+}]_i$ were calculated, averaged, and expressed as mean $\Delta F/F$ (see Materials and Methods). *C*, Mean change in $[Ca^{2+}]_i$ for eight randomly selected cells from a P2 neocortical slice after application of 30 μM muscimol (*squares*). After a 30 min recovery period, a second muscimol application, in the presence of 500 μM Cd^{2+}, failed to elicit $[Ca^{2+}]_i$ increases in the same cells (*circles*).

cells shifted an average of 8.1 ± 0.9 mV more negative in the presence of furosemide, consistent with a dependence of the muscimol response on a high $[Cl^-]_i$ maintained by a Cl^- transport process (Fig. 4*C*). Taken together, these data indicate that the $GABA_A$ reversal potential is mediated predominantly by Cl^- flux in embryonic and neonatal cortical neurons. These findings allow use of the Nernst equation to estimate $[Cl^-]_i$ in embryonic and neonatal cells based on the GABA and muscimol-reversal potential data (Fig. 3*B*).

$GABA_A$ receptor activation increases $[Ca^{2+}]_i$ by activating VGCCs

One possible consequence of membrane depolarization could be an increase in $[Ca^{2+}]_i$ mediated by the activation of VGCCs. Previous results from our laboratory have demonstrated that GABA application produces increases in $[Ca^{2+}]_i$ in embryonic VZ cells (LoTurco et al., 1995). In light of the present analysis of the $GABA_A$ reversal potential, we extended our Ca^{2+} imaging studies to embryonic CP and early postnatal neocortical cells. Figure 5*A1–A3* shows that muscimol (30 μM) application produced a reversible increase in $[Ca^{2+}]_i$ in CP cells at E17. Eight cells were randomly chosen from the microscopic field, and the increases in $[Ca^{2+}]_i$ were calculated and expressed as $\Delta F/F$ (see Materials and Methods); these results are shown in Figure 5*B*. Similarly, increases in $[Ca^{2+}]_i$ were found in early postnatal neocortical cells. Figure 5*C* shows the mean change in $[Ca^{2+}]_i$ for eight cells from a P2 neocortical slice after application of 30 μM muscimol. After a 30 min recovery period, a second muscimol application, in the presence of 500 μM Cd^{2+}, failed to elicit $[Ca^{2+}]_i$ increases in the same cells, suggesting that the $GABA_A$ receptor-mediated increase in $[Ca^{2+}]_i$ results from the activation of VGCCs. A similar level of blockade was found when using 30 μM La^{3+} (data not shown). These results are consistent with $GABA_A$-mediated increases in $[Ca^{2+}]_i$ reported in similar studies carried out in developing rat visual cortex (Yuste and Katz, 1991; Lin et al., 1994).

sPSCs and $[Ca^{2+}]_i$ increases are $GABA_A$-mediated

Under conditions of whole-cell recording, spontaneous synaptic activity was observed in neocortical neurons. In 25 recordings from P1–P4 slices, 72.0% of the cells had resolvable sPSCs. The sPSCs were not blocked when the non-NMDA receptor antagonist CNQX (10 μM) was present in the bath solution (n = 12). However, in the continued presence of CNQX, the sPSCs were abolished when BMI (10 μM) was applied focally (n = 9) (Fig. 6*A*) but not when the NMDA receptor antagonist AP-5 (100 μM) was applied (n = 7). This suggests that the majority of the early postnatal sPSCs are mediated by activation of $GABA_A$ receptors. TTX (2 μM) also could eliminate the sPSCs, indicating that they are action potential-dependent (n = 3). We compared the reversal potential of the muscimol-induced current with the reversal potential of the $GABA_A$-mediated sPSC in three cells. An example from a P4 neocortical neuron is shown in Figure 6. sPSCs were collected at each of five membrane potentials ranging from −80 mV to 40 mV. Fifteen to 30 sPSCs at each membrane potential were averaged, and the peak current was plotted. The approximate reversal potential for the averaged sPSCs was −4.1 mV (Fig. 6*B*), whereas E_{GABA_A} was found to be −5.4 mV (Fig. 6*C*). Both

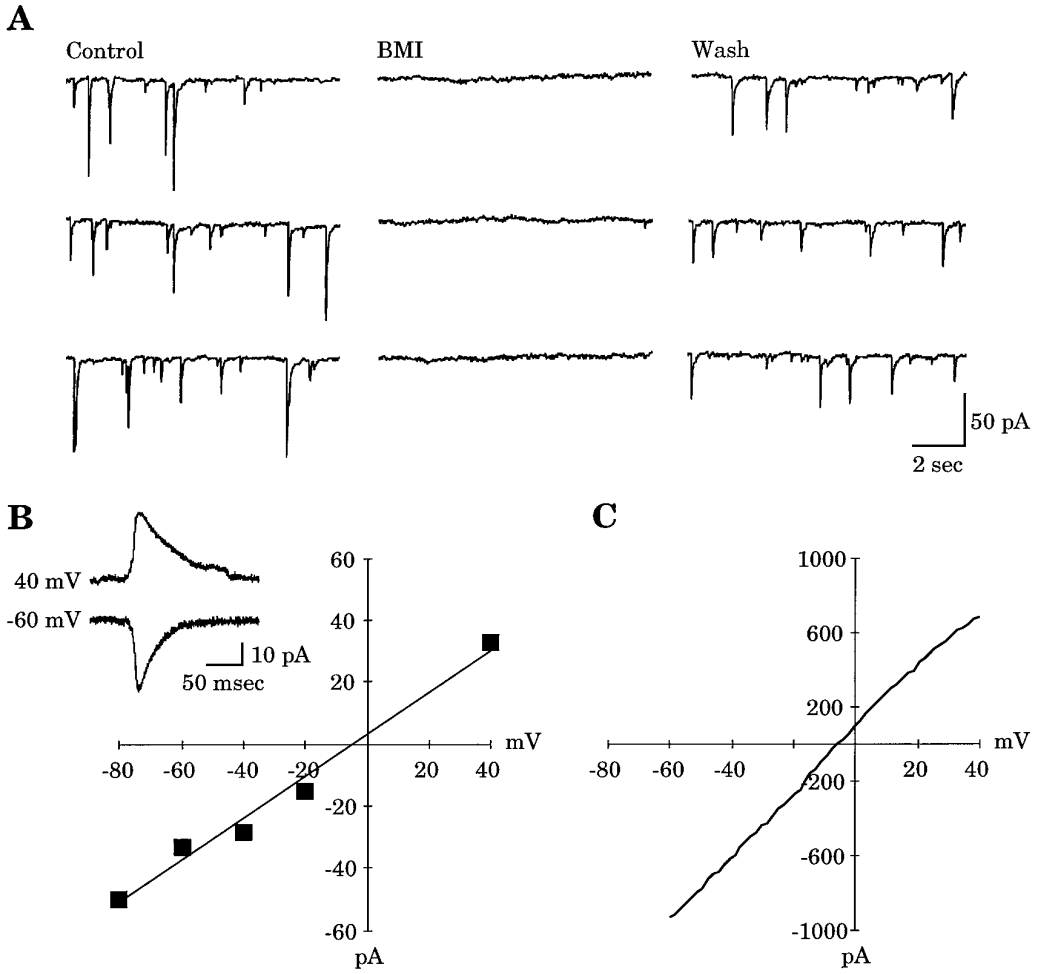

Figure 6. Activation of $GABA_A$ receptors by both endogenously released GABA and exogenously applied muscimol (30 μM) yields similar reversal potentials. *A*, Examples of sPSCs recorded in control conditions (*Control*), during 10 μM BMI application (*BMI*), and after BMI was washed out (*Wash*). Application of AP-5 (100 μM) did not abolish the sPSCs (data not shown). All recordings are in the presence of 10 μM CNQX in the bath solution. $V_h = -60$ mV. *B*, *I–V* curve derived from averaged sPSCs at five membrane potentials with an approximate reversal potential of −4.1 mV. *Inset* shows averaged sPSCs at two membrane potentials. *C*, The muscimol induced *I–V* curve for the same cell as show in *B*, with an E_{GABA_A} of −5.4 mV.

of these values are close to that predicted by the Nernst equation for the experimentally established Cl^- gradient (i.e., −6.2 mV). This demonstrates that the reversal potential for an endogenously active $GABA_A$-mediated synaptic current is nearly identical to the reversal potential for the exogenously applied $GABA_A$ agonist muscimol.

Given the $GABA_A$ reversal potentials determined above with perforated patches, spontaneous $GABA_A$-mediated synaptic potentials could depolarize neonatal neurons sufficiently to activate VGCC and increase $[Ca^{2+}]_i$. To test this idea directly, slices of early postnatal neocortex were imaged using confocal laser microscopy. Figure 7*A* shows the Ca^{2+} transients in a P1 neocortical cell. When BMI (30 μM) was washed into the recording chamber, the spontaneous events were reversibly blocked. Furthermore, TTX (2 μM) also could block the spontaneous increases in $[Ca^{2+}]_i$, consistent with our physiological findings that TTX can eliminate the BMI-sensitive sPSCs. Finally, muscimol (30 μM) application produced an increase in the $[Ca^{2+}]_i$ in the same cell, indicating the presence of $GABA_A$ receptors on this cell and confirming their ability to produce $[Ca^{2+}]_i$ increases. Similar data were obtained for neocortical cells at P3 (Fig. 7*B*). At P3, we found that BMI blocked the spontaneous $[Ca^{2+}]_i$ increases in 77.8% ($n = 18$) of the cells, and in 100% of these cells, muscimol application produced increases in $[Ca^{2+}]_i$. These results, in combination with the $GABA_A$ reversal potentials determined with perforated patches, suggest that in the early postnatal neocortex, spontaneous $GABA_A$-mediated depolarizing potentials produce $[Ca^{2+}]_i$ increases, presumably by the activation of VGCCs.

DISCUSSION

Depolarizing effects of GABA have been reported in immature cells from a number of brain regions including the neocortex (Luhmann and Prince, 1991), hippocampus (Ben-Ari et al., 1989; Cherubini et al., 1990), spinal cord (Wu et al., 1992; Reichling et al., 1994; Wang et al., 1994; Rohrbough and Spitzer, 1996), cerebellum (Connor et al., 1987), olfactory bulb (Serafini et al., 1995), and retina (Yamashita and Fukuda, 1993). In cortical neurons, most of these studies have been performed using sharp intracellular electrodes, but these methods cannot be applied to very immature neurons without causing significant injury. Furthermore, one cannot assume that the intracellular ionic composition is completely intact with sharp electrode recording. Whole-cell voltage-clamp techniques are

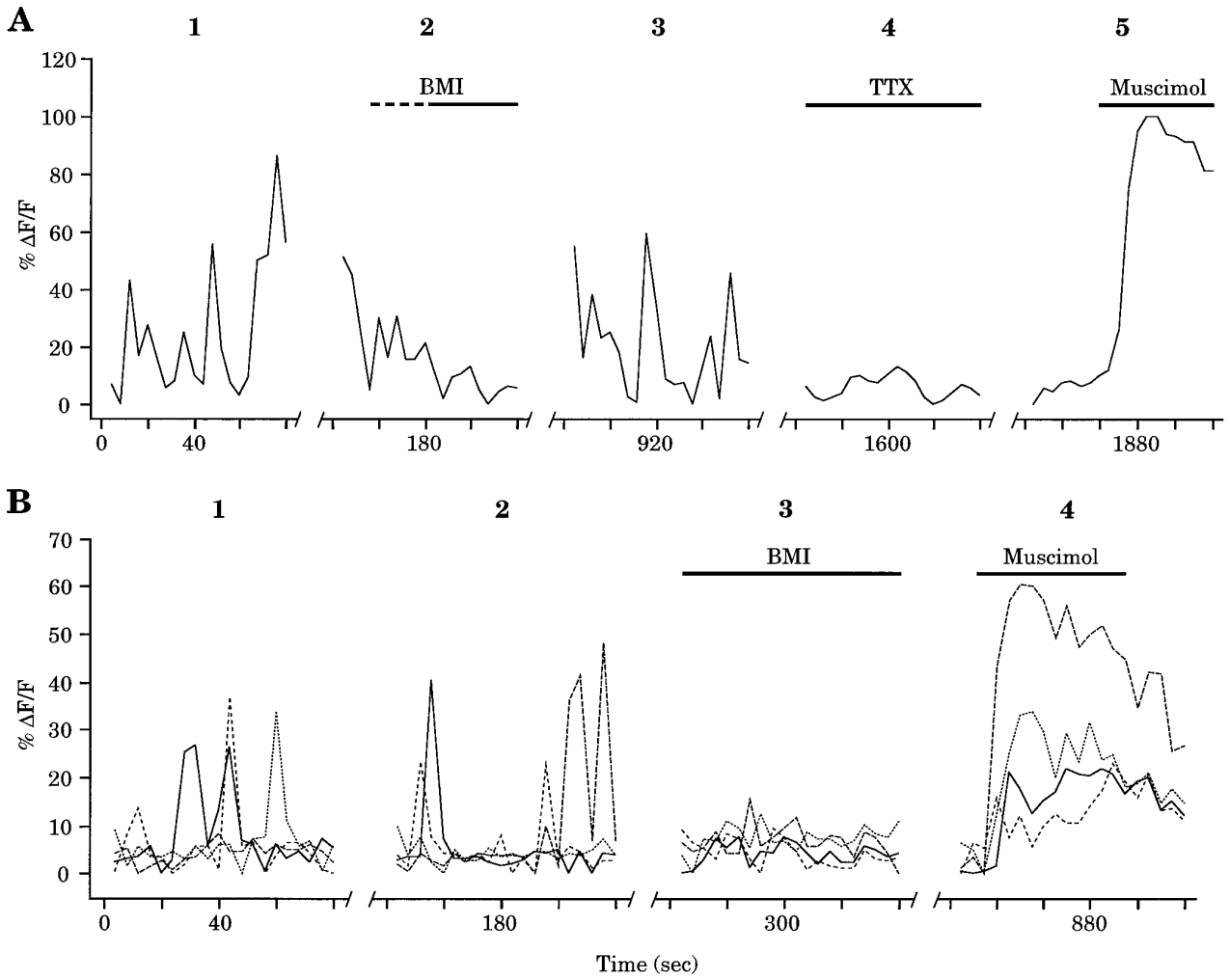

Figure 7. Spontaneous increases in $[Ca^{2+}]_i$ in postnatal neocortical cells are mediated by $GABA_A$ receptor activation. *A*, Spontaneous Ca^{2+} transients in a P1 neocortical cell (*1*) were reversibly blocked by BMI (30 μM) (*2*, *3*). TTX (2 μM) also could eliminate the spontaneous increases in $[Ca^{2+}]_i$ (*4*). *2* Shows activity during wash in of bicuculline (indicated by the *dashed line*), whereas *4* shows activity 3 min after wash in of TTX. The muscimol (30 μM)-mediated increase in $[Ca^{2+}]_i$ (*5*) suggests the presence of $GABA_A$ receptors on this cell. Breaks in the *x*-axis represent ~1, 10, 10, and 3 min, respectively. *B*, Combined data from four P3 neocortical cells. Each cell had at least one spontaneous increase in $[Ca^{2+}]_i$ during two control recording periods (*1*, *2*). In the presence of BMI, no additional spontaneous increases in $[Ca^{2+}]_i$ were observed (*3*). BMI application began ~1 min before data acquisition. As in *A*, muscimol (30 μM) application also produced $[Ca^{2+}]_i$ increases (*4*). Breaks in the *x*-axis represent ~1, 1, and 8 min, respectively.

well-suited to recording from small, fragile cells, but because cell contents exchange with the electrode solution under whole-cell conditions, ion gradients across the cell membrane are severely biased toward the pipette solution. The use of perforated-patch recordings with an anion-impermeant ionophore (Abe et al., 1994; Ebihara et al., 1995; Kyrozis and Reichling, 1995) overcomes these limitations and allows accurate measurements of E_{GABA_A} in small, immature cells. We have applied this technique to examine developmental changes in E_{GABA_A} in neocortical cells *in situ*. The results show that E_{GABA_A} becomes more negative as cells mature, with the most positive values observed in the youngest cortical precursor cells. The measured resting potentials of these immature cells verify that $GABA_A$ receptor activation would function to depolarize neurons during early development, and the depolarization appears to be determined largely by the Cl^- gradient, with the highest $[Cl^-]_i$ found in embryonic cortical precursor cells and the $[Cl^-]_i$ gradually decreasing as neurons mature.

The mechanism of GABA depolarization may differ between immature and adult cortical neurons

The depolarization mediated by GABA in developing cortical cells contrasts, in some regards, with the GABA-mediated depolarization found, under certain conditions, in adult cortical neurons (Alger and Nicoll, 1982; Connors et al., 1988; Janigro and Schwartzkroin, 1988; Lambert et al., 1991; Grover et al., 1993; Staley et al., 1995). In adult cells, $GABA_A$ receptor activation by either high-frequency stimulation or exogenous application of large amounts of GABA can produce a biphasic response of hyperpolarization followed by depolarization (Connors et al., 1988; Grover et al., 1993; Staley et al., 1995). In this case, a bicarbonate conductance appears to play a significant role in the depolarizing phase of the response (Staley et al., 1995); however, other mechanisms have been proposed (Deisz and Luhmann, 1995). In the present study, responses to exogenously applied GABA or muscimol were monophasic; even with prolonged agonist application, we never saw multiphasic responses, except at the

very latest time point studied (i.e., P16). Furthermore, in bicarbonate-free saline, we observed inward currents when muscimol was applied to E19 CP cells voltage-clamped close to the resting membrane potential. This contrasts with results found in adult neocortical (Staley et al., 1995) and hippocampal (Grover et al., 1993) pyramidal neurons in which GABA application to the distal dendrites did not produce inward current or membrane depolarization when recording in bicarbonate-free saline. These results lead us to believe that the $GABA_A$-mediated depolarization in adult and developing neocortical cells may be mechanistically distinct and that the Cl^- gradient is primarily responsible for GABA-mediated depolarization in developing cells. This is consistent with other developmental studies in immature spinal cord neurons in which $GABA_A$-mediated depolarization has been shown to be primarily attributable to the Cl^- gradient (Reichling et al., 1994; Rohrbough and Spitzer, 1996). Furthermore, evidence has suggested that immature neocortical neurons have less efficient Cl^- transport in the outward direction (Luhmann and Prince, 1991), which can account for higher $[Cl^-]_i$ and more positive $GABA_A$ reversal potentials. Likewise, measurements of the $[Cl^-]_i$ in cultured hippocampal neurons have demonstrated that more immature cells have higher somatic $[Cl^-]_i$ (Hara et al., 1992).

GABA may influence cortical development through Ca^{2+}-dependent mechanisms

$GABA_A$-mediated spontaneous synaptic potentials can occur early in postnatal development in both the neocortex and hippocampus (Luhmann and Prince, 1991; Hosokawa et al., 1994). In the neocortex, BMI-sensitive spontaneous synaptic events can precede evoked GABAergic synaptic potentials (Luhmann and Prince, 1991). Furthermore, in immature hippocampal neurons in slices, BMI application has been shown to induce small hyperpolarizations in membrane potential, suggesting that tonic GABA release can influence the resting membrane potential (Ben-Ari et al., 1989; Hosokawa et al., 1994). Likewise, hippocampal neurons in cell culture have been shown to tonically release GABA by an action potential-independent mechanism (Valeyev et al., 1993). The early maturation of GABA release mechanisms as well as the early development of spontaneous $GABA_A$-mediated synaptic events well before development of synaptic inhibition supports the notion that GABA has a functional role in nervous system development. GABA even may have an influence on the key processes of proliferation, migration, and differentiation. Recently, GABA has been shown to influence DNA synthesis in cortical precursor cells through activation of $GABA_A$ receptors (LoTurco et al., 1995). In addition, GABA has been shown to have a variety of effects on the migratory behavior of young postmitotic neurons grown in tissue culture (Behar et al., 1994, 1996). Also, GABA has been shown to induce morphological changes (Barbin et al., 1993) and alter neurotrophic factor expression (Berninger et al., 1995) in cultured hippocampal neurons.

Many of the trophic actions of GABA in cortical cells may be mediated by calcium-dependent mechanisms. In this study, as well as others (Yuste and Katz, 1991; Lin et al., 1994; LoTurco et al., 1995), exogenous GABA or muscimol application has been shown to increase $[Ca^{2+}]_i$ in immature neocortical cells through the activation of VGCCs. We have demonstrated that BMI application can reversibly block spontaneous increases in $[Ca^{2+}]_i$ in early postnatal neocortical neurons, suggesting that spontaneous $GABA_A$-mediated synaptic potentials may depolarize cells sufficiently to activate VGCCs. This is likely to be an age-related phenomenon, because synaptic $GABA_A$ receptor activation has been shown to increase $[Ca^{2+}]_i$ in P2–P5 but not P12–P13 hippocampal neurons (Leinekugel et al., 1995). We have not characterized the type(s) of VGCC expressed by immature cortical neurons, but it has been suggested that low-threshold VGCCs are responsible for GABA-induced $[Ca^{2+}]_i$ increases in these cells (Yuste and Katz, 1991). Calcium entry via GABA-mediated VGCC activation has been shown to upregulate brain-derived neurotrophic factor (BDNF) expression in immature hippocampal neurons (Berninger et al., 1995). In cultured embryonic cortical neurons, activation of VGCCs but not glutamate channels increased neuronal survival, an effect that correlated with increased BDNF expression (Ghosh et al., 1994). Finally, muscimol application has been found to regulate the phenotype of immature hippocampal interneurons, an effect that may be mediated through the regulation of BDNF expression and release from target cells (Marty et al., 1996). There is mounting evidence that GABA may act as a trophic factor in early development by depolarizing cells, activating VGCCs, and, in turn, regulating gene expression through the activation of Ca^{2+}-dependent second messenger pathways.

As shown in this study, GABA continues to have depolarizing effects at early postnatal stages. The transient BMI-sensitive spontaneous $[Ca^{2+}]_i$ increases observed in neonatal cortical slices reported here may represent the activity of early-forming GABAergic synapses. The potential for early GABAergic synapses to depolarize postsynaptic cells and activate Ca^{2+} entry raises the possibility that the establishment or strengthening of inhibitory synapses may involve similar mechanisms to those involved in the formation of activity-dependent excitatory contacts (Constantine-Paton et al., 1990; Cline, 1991). Recent evidence in adult hippocampus has suggested that $GABA_A$ receptor-mediated depolarization is able to increase the conductance of the NMDA receptor, possibly by relieving the Mg^{2+} block of the channel (Staley et al., 1995). Furthermore, a novel form of GABA-dependent long-lasting potentiation has been reported in the hippocampus of genetically altered mice (Frey et al., 1996). Thus, it appears that GABA may play a role in adult forms of synaptic plasticity and also may regulate plastic events during development.

REFERENCES

Abe Y, Furukawa K, Itoyama Y, Akaike N (1994) Glycine response in acutely dissociated ventromedial hypothalamic neuron of the rat: new approach with gramicidin perforated patch-clamp technique. J Neurophysiol 72:1530–1537.

Alger BE, Nicoll RA (1982) Pharmacological evidence for two kinds of GABA receptor on rat hippocampal pyramidal cells studied *in vitro*. J Physiol (Lond) 328:125–141.

Andersen P, Dingledine R, Gjerstad J, Langmoen IA, Lauresen AM (1980) Two different responses of hippocampal pyramidal cells to application of gamma-amino butyric acid. J Physiol (Lond) 305:279–296.

Araki T, Kiyama H, Tohyama M (1992) $GABA_A$ receptor subunit messenger RNAs show differential expression during cortical development in the rat brain. Neuroscience 51:583–591.

Barbin G, Pollard H, Gaiarsa JL, Ben-Ari Y (1993) Involvement of $GABA_A$ receptors in the outgrowth of cultured hippocampal neurons. Neurosci Lett 152:150–154.

Behar TN, Schaffner AE, Colton CA, Somogyi R, Olah Z, Lehel C, Barker JL (1994) GABA-induced chemokinesis and NGF-induced chemotaxis of embryonic spinal cord neurons. J Neurosci 14:29–38.

Behar TN, Li Y, Tran HT, Ma W, Dunlap V, Scott C, Barker JL (1996) GABA stimulates chemotaxis and chemokinesis of embryonic cortical neurons via calcium-dependent mechanisms. J Neurosci 16:1808–1818.

Ben-Ari Y, Cherubini E, Corradetti R, Gaiarsa JL (1989) Giant synaptic potentials in immature rat CA3 hippocampal neurones. J Physiol (Lond) 416:303–325.

Berninger B, Marty S, Zafra F, da Penha Berzaghi M, Thoenen H (1995) GABAergic stimulation switches from enhancing to repressing BDNF expression in rat hippocampal neurons during maturation *in vitro*. Development 121:2327–2335.

Blanton MG, LoTurco JJ, Kriegstein AR (1989) Whole cell recording from neurons in slices of reptilian and mammalian cerebral cortex. J Neurosci Methods 30:203–210.

Bormann J, Hamill OP, Sakmann B (1987) Mechanism of anion permeation through channels gated by glycine and γ-aminobutyric acid in mouse cultured spinal neurones. J Physiol (Lond) 385:243–286.

Cherubini E, Rovira C, Gaiarsa JL, Corradetti R, Ben-Ari Y (1990) GABA mediated excitation in immature rat CA3 hippocampal neurons. Int J Dev Neurosci 8:481–490.

Cline HT (1991) Activity-dependent plasticity in the visual systems of frogs and fish. Trends Neurosci 14:104–111.

Connor JA, Hsiu-Yu T, Hockberger P (1987) Depolarization- and transmitter-induced changes in intracellular Ca^{2+} of rat cerebellar granule cells in explant cultures. J Neurosci 7:1384–1400.

Connors BW, Benardo LS, Prince DA (1983) Coupling between neurons of the developing rat neocortex. J Neurosci 3:773–782.

Connors BW, Malenka RC, Silva LR (1988) Two inhibitory postsynaptic potentials, and $GABA_A$ and $GABA_B$ receptor-mediated responses in neocortex of rat and cat. J Physiol (Lond) 406:443–468.

Constantine-Paton M, Cline HT, Debski E (1990) Patterned activity, synaptic convergence, and the NMDA receptor in developing visual pathways. Annu Rev Neurosci 13:129–154.

Deisz RA, Luhmann HS (1995) Development of cortical excitation and inhibition. In: The cortical neuron (Gutnick MJ, Mody I, eds), pp 230–246. New York: Oxford UP.

Ebihara S, Shirato K, Harata N, Akaike N (1995) Gramicidin-perforated patch recording: GABA response in mammalian neurones with intact intracellular chloride. J Physiol (Lond) 434:77–86.

Frey U, Muller M, Kuhl D (1996) A different form of long-lasting potentiation revealed in tissue plasminogen activator mutant mice. J Neurosci 16:2057–2063.

Ghosh A, Carnahan J, Greenberg ME (1994) Requirement for BDNF in activity-dependent survival of cortical neurons. Science 263:1618–1823.

Grover LM, Lambert NA, Schwartzkroin PA, Teyler TJ (1993) Role of HCO_3^- ions in depolarizing $GABA_A$ receptor-mediated responses in pyramidal cells of rat hippocampus. J Neurophysiol 69:1541–1555.

Hara M, Inoue M, Yasukura T, Ohnishi S, Mikami Y, Inagaki C (1992) Uneven distribution of intracellular Cl^- in rat hippocampal neurons. Neurosci Lett 143:135–138.

Hladky SB, Haydon DA (1972) Ion transfer across lipid membranes in the presence of gramicidin A. I. Studies of the unit conductance channel. Biochim Biophys Acta 274:294–312.

Horn R, Marty A (1988) Muscarinic activation of ionic currents measured by a new whole-cell recording method. J Gen Physiol 92:145–159.

Hosokawa Y, Sciancalepore M, Stratta F, Martina M, Cherubini E (1994) Developmental changes in spontaneous $GABA_A$-mediated synaptic events in rat hippocampal CA3 neurons. Eur J Neurosci 6:805–813.

Janigro D, Schwartzkroin PA (1988) Effects of GABA and baclofen on pyramidal cells in the developing rabbit hippocampus: an "*in vitro*" study. Brain Res 469:171–184.

Kaila K, Voipio J (1987) Postsynaptic fall in intracellular pH induced by GABA-activated bicarbonate conductance. Nature 330:163–165.

Kaila K, Pasternack M, Saarikoski J, Voipio J (1989) Influence of GABA-gated bicarbonate conductance on potential, current and intracellular chloride in crayfish muscle fibres. J Physiol (Lond) 416:161–181.

Kyrozis A, Reichling DB (1995) Perforated-patch recording with gramicidin avoids artifactual changes in intracellular chloride concentration. J Neurosci Methods 57:27–35.

Lambert NA, Borroni AM, Grover LM, Teyler TJ (1991) Hyperpolarizing and depolarizing $GABA_A$ receptor-mediated dendritic inhibition in area CA1 of the rat hippocampus. J Neurophysiol 66:1538–1548.

Laurie DJ, Wisden W, Seeburg PH (1992) The distribution of thirteen $GABA_A$ receptor subunit mRNAs in the rat brain. III. Embryonic and postnatal development. J Neurosci 12:4151–4172.

Leinekugel X, Tseeb V, Ben-Ari Y, Bregestovski P (1995) Synaptic $GABA_A$ activation induces Ca^{2+} rise in pyramidal cells and interneurons from rat neonatal hippocampal slices. J Physiol (Lond) 487:319–329.

Lin M-H, Takahashi MP, Takahashi Y, Tsumoto T (1994) Intracellular calcium increase induced by GABA in visual cortex of fetal and neonatal rats and its disappearance with development. Neurosci Res 20:85–94.

LoTurco JJ, Kriegstein AR (1991) Clusters of coupled neuroblasts in embryonic neocortex. Science 252:563–566.

LoTurco JJ, Owens DF, Heath MJS, Davis MBE, Kriegstein AR (1995) GABA and glutamate depolarize cortical progenitor cells and inhibit DNA synthesis. Neuron 15:1287–1298.

Luhmann HJ, Prince DA (1991) Postnatal maturation of the GABAergic system in rat neocortex. J Neurophysiol 65:247–263.

Marty A, Finkelstein A (1975) Pores formed in lipid bilayer membranes by nystatin: differences in its one-sided and two-sided action. J Gen Physiol 95:515–526.

Marty S, Berninger B, Carroll P, Thoenen H (1996) GABAergic stimulation regulates the phenotype of hippocampal interneurons through the regulation of brain-derived neurotrophic factor. Neuron 16:565–570.

Myers VB, Haydon DA (1972) Ion transfer across lipid membranes in the presence of gramicidin A. II. The ion selectivity. Biochim Biophys Acta 274:313–322.

Neher E (1992) Correction of liquid junction potentials in patch clamp experiments. Methods Enzymol 207:123–131.

Peinado A, Yuste R, Katz LC (1993) Extensive dye coupling between rat neocortical neurons during the period of circuit formation. Neuron 10:103–114.

Poulter MO, Barker JL, O'Carroll AM, Lolait SJ, Mahan LC (1992) Differential and transient expression of $GABA_A$ receptor alpha-subunit mRNAs in the developing rat CNS. J Neurosci 12:2888–2900.

Reichling DB, MacDermott AB (1991) Lanthanum actions on excitatory amino acid-gated currents and voltage-gated calcium currents in rat dorsal horn neurons. J Physiol (Lond) 441:199–218.

Reichling DB, Kyrozis A, Wang J, MacDermott AB (1994) Mechanisms of GABA and glycine depolarization-induced calcium transients in rat dorsal horn neurons. J Physiol (Lond) 476:411–421.

Rohrbough J, Spitzer NC (1996) Regulation of intracellular Cl^- levels by Na^+-dependent Cl^- cotransport distinguishes depolarizing from hyperpolarizing $GABA_A$ receptor-mediated responses in spinal neurons. J Neurosci 16:82–91.

Serafini R, Valeyev AY, Barker JL, Poulter MO (1995) Depolarizing GABA-activated Cl^- channels in embryonic rat spinal and olfactory bulb cells. J Physiol (Lond) 488:371–386.

Staley KJ, Soldo BL, Proctor WR (1995) Ionic mechanisms of neuronal excitation by inhibitory $GABA_A$ receptors. Science 269:977–981.

Valeyev AY, Cruciani RA, Lange CD, Smallwood VS, Barker JL (1993) Cl^- channels are randomly activated by continuous GABA secretion in cultured embryonic rat hippocampal neurons. Neurosci Lett 155:199–203.

Wang J, Reichling DB, Kyrozis A, MacDermott AB (1994) Developmental loss of GABA- and glycine-induced depolarization and Ca^{2+} transients in embryonic rat dorsal horn neurons in culture. Eur J Neurosci 6:1275–1280.

Wu W, Ziskind-Conhaim L, Sweet M (1992) Early development of glycine and GABA-mediated synapses in rat spinal cord. J Neurosci 12:3935–3945.

Yamashita M, Fukuda Y (1993) Calcium channels and GABA receptors in the early embryonic chick retina. J Neurobiol 24:1600–1614.

Yuste R, Katz LC (1991) Control of postsynaptic Ca^{2+} influx in developing neocortex by excitatory and inhibitory neurotransmitters. Neuron 6:333–344.